Chirality sorting using two-wave-interference–induced lateral optical force

Huajin Chen,[1,2,*] Chenghua Liang,[2] Shiyang Liu,[3,1] and Zhifang Lin[1,4,5]

[1]*State Key Laboratory of Surface Physics (SKLSP) and Department of Physics, Fudan University, Shanghai 200433, China*

[2]*School of Electrical and Information Engineering, Guangxi University of Science and Technology, Liuzhou, Guangxi 545006, China*

[3]*Institute of Information Optics, Zhejiang Normal University, Jinhua, Zhejiang 321004, China*

[4]*Key Laboratory of Micro and Nano Photonic Structures (MOE), Fudan University, Shanghai 200433, China*

[5]*Collaborative Innovation Center of Advanced Microstructures, Fudan University, Shanghai 200433, China*

(Received 13 April 2016; published 26 May 2016)

We demonstrate that a lateral optical force (LOF) can be induced on chiral nanoparticles immersed in the two interfering plane waves. The LOF can push the chiral nanoparticle sideways, in the direction relying on the helicity of the particle as well as the phase difference between two waves. Analytical theory reveals that the LOF comes mostly from the direct coupling of the optical vorticity with the particle chirality. In particular, the LOF has a magnitude comparable to the gradient force and radiation pressure when the particle chirality is sufficiently large. The LOF may serve for chirality sorting due to its unusual properties and also provide an opportunity for passive chiral spectroscopy.

DOI: 10.1103/PhysRevA.93.053833

I. INTRODUCTION

Chirality describes the geometric characteristic of an object that is not superimposable on its mirror image by translations or rotations [1]; for example, the two human hands. It plays a fundamental role in physics [2], chemistry [3], biology [4], and biomedicine [5], but detecting and separating it remains challenging, especially in the pharmaceutical industry [6,7]. Although a great number of chiral separation approaches [8], such as liquid-liquid extraction and distillation, are proposed for separating chiral substances, they might destroy the biomolecules and cells due to their essential dependence on the differences in solubilities or boiling points. With the advent of laser beams, optical forces based on a great variety of optical fields have been widely used in passive manipulation of chiral molecules [9,10] and chiral droplets [11,12]. Recently, it was shown that a linearly polarized plane wave can exert an anomalous lateral optical force (LOF) on a chiral particle above a substrate. Such force can push the particle with opposite helicities in opposite direction [13] and thus offer a possibility to sort and separate chiral molecules or enantiomers. The LOF acting on a nonchiral particle above a substrate [14] or located at a water-air interface [15] immersed in circularly polarized plane waves has been subsequently reported. Also, for an incident evanescent wave, a chiral particle near a substrate can be subject to a LOF, which is attributed to the direct coupling between the transverse spin angular momentum (SAM) and the particle chirality [16]. However, these theoretical proposals suggest that the occurrence of LOFs must require a substrate to reflect the incident waves or generate the evanescent waves, somewhat limiting the freedom in optical manipulations.

In this paper, we demonstrate that a simple optical field—two interfering plane waves—can also exert a LOF on chiral particles in vacuum. The LOF acts in a direction in which there is neither an intensity gradient nor wave propagation. Such LOFs can move the chiral particle sideways, with its direction dependent on both the handedness of the particle and the phase difference between two plane waves, enabling the flexible tunability. The physical origin of the LOF can be derived from the analytical expressions of optical forces within the dipole approximation, residing in the interaction of the optical vorticity with the particle chirality. These features of the LOF may find applications in sorting and separation of chiral particles.

II. RESULTS AND DISCUSSION

We investigate the lateral chirality-sorting force by calculating the y component of the optical force on a small chiral nanoparticle immersed in the interference field of two plane waves, as schematically illustrated in Fig. 1(a). The two linearly polarized plane waves propagate along wave vectors $\mathbf{k}_{12} = k_0(\hat{\mathbf{z}}\cos\alpha \pm \hat{\mathbf{x}}\sin\alpha)$ and their electric fields can be written as $\mathbf{E}_{12} = E_0(\cos\alpha\ \hat{\mathbf{x}} \mp \sin\alpha\ \hat{\mathbf{z}})e^{ik_0(z\cos\alpha \pm x\sin\alpha)}$, with the two signs corresponding to the indices 1 and 2. E_0 is the amplitude of electric fields and k_0 is the wave number in vacuum. Here, the time dependence $e^{-i\omega t}$ is assumed and suppressed. For a chiral particle, the constitutive relations are given by [17–19]

$$\begin{aligned}\mathbf{D} &= \varepsilon_0\varepsilon\mathbf{E} + i\kappa\sqrt{\varepsilon_0\mu_0}\mathbf{H},\\ \mathbf{B} &= -i\kappa\sqrt{\varepsilon_0\mu_0}\mathbf{E} + \mu_0\mu\mathbf{H},\end{aligned} \tag{1}$$

where ε_0 and μ_0 are the permittivity and permeability in vacuum, ε and μ are the relative permittivity and permeability of the chiral particle, and κ is the chirality parameter, controlled by the inequality $\kappa < \sqrt{\varepsilon\mu}$ [19,20]. The dispersion relations for a plane wave in such a medium are $k_1 = k_0(\sqrt{\varepsilon\mu} + \kappa)$ and $k_2 = k_0(\sqrt{\varepsilon\mu} - \kappa)$, corresponding to two circularly polarized states of light. As an example of the LOF, we assume that the two waves have the same incident wavelength of $\lambda = 1.064\ \mu$m and incident angle of $\alpha = 45^\circ$ throughout this paper, unless otherwise stated. By using the full-wave simulation (FWS) based on the generalized Mie scattering theory [21] and the Maxwell stress tensor [22], the y component of the time-averaged optical force F_y acting on nanoparticles is exactly calculated as functions of the particle displacement along the x axis, as shown in Fig. 1(b). It is evident that the conventional particle with $\kappa = 0$ is not subject to any LOF,

*huajinchen13@fudan.edu.cn

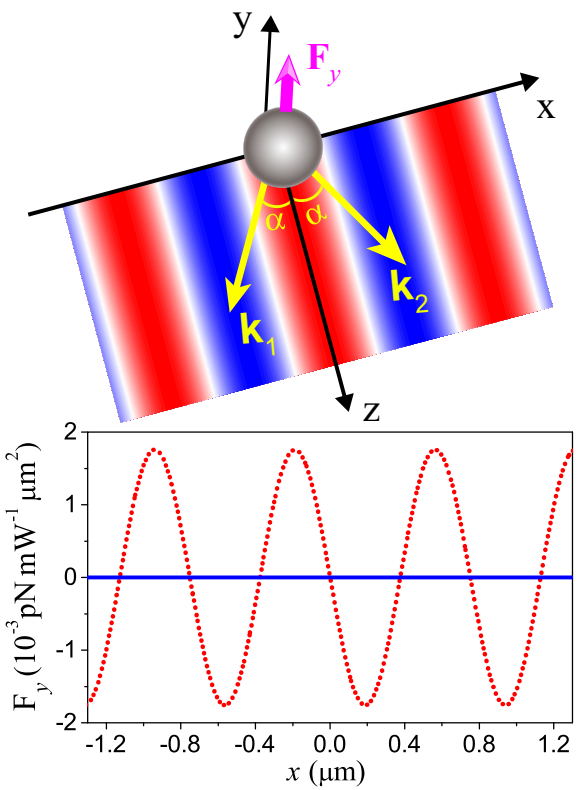

FIG. 1. (a) Schematic illustration of a LOF on a chiral particle immersed in the interference field of two plane waves. (b) The LOF F_y on a nanoparticle versus the particle displacement along the x axis obtained from the FWS. The blue and red lines denote the particle with $k = 0$ and $k = 0.3$, respectively. The two plane waves have the same incident wavelength of $\lambda = 1.064$ μm and incident angle of $\alpha = 45^\circ$. The particle has the radius $r_s = 0.1$ μm, $\varepsilon = 2.53$, and $\mu = 1$ for the above cases.

while a LOF appears on the chiral particle with $\kappa = 0.3$, as illustrated by the blue and red lines, respectively. Here we take the chiral parameter $\kappa = 0.3$ only as an example to illustrate the crucial role of the chiral effect for the realization of the LOF, and in the experiment the chiral particle can be a spherical particle made from chiral material [23], e.g., a cholesteric liquid crystal spherical droplet [11,12]. We can observe from Fig. 1(b) that the LOF changes its signs with the particle displacement x and also experiences an oscillation with period $\lambda/\sqrt{2}$ because the phase difference of $\phi = 2k_0 x \sin\alpha$ between two waves determines the interference intensity. In addition, we also note that a similar LOF appears on a gold Mie particle in the two-wave inference field, which arises from the interaction between higher-order multipoles [24]. In that case, however, one needs a nonvanishing electric field in the x, y, and z directions, whereas for our case the LOF can be induced even when the electric field is polarized in the x-z plane, without explicitly breaking the symmetry with respect to $y = 0$, showing the significant role of the particle chirality. It is noted that the LOF due to the two-wave interference also exists for a particle with geometric chirality like a gold helix, since the latter shares the same underlying physics as the spherical chiral particle [13].

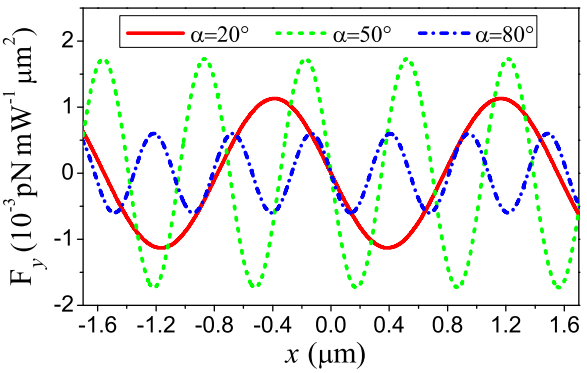

FIG. 2. LOF F_y on a chiral particle with $\kappa = 0.3$ versus the particle displacement along the x axis. The red, green, and blue lines denote the two plane waves with incident angles $\alpha = 20^\circ$, 50°, and 80°, respectively. Other parameters are the same as those in Fig. 1.

The LOF on the chiral particle also exists for the two plane waves with other nonzero incident angles α, as shown in Fig. 2 for the cases with $\alpha = 20^\circ$, $\alpha = 50^\circ$, and $\alpha = 80^\circ$, where all other parameters are the same as those in Fig. 1. We can clearly see that the LOFs occur with different magnitudes and also oscillate with different periods $\lambda/(2\sin\alpha)$ determined by the phase difference between two waves. By comparing with Fig. 1, we also find that the LOF for the case with $\alpha = 45^\circ$ has the largest amplitude and it can thus be chosen as a typical example to examine the physical origin and properties of the LOF in the discussion below.

To trace the origin of the LOF, we analytically derive the optical force within the dipole approximation owing to the small size of the chiral particle compared with the wavelength. Accordingly, the time-averaged optical force on a chiral particle can be expressed in terms of the electric and magnetic dipole moments [25,26]:

$$\langle \mathbf{F} \rangle = \frac{1}{2}\mathrm{Re}\left[(\nabla \mathbf{E}^*)\cdot\mathbf{p} + (\nabla \mathbf{B}^*)\cdot\mathbf{m} - \frac{k_0^4}{6\pi\varepsilon_0 c}(\mathbf{p}\times\mathbf{m}^*)\right], \tag{2}$$

where c is the speed of light in vacuum, and $\mathbf{E}$ and $\mathbf{B}$ are the fields acting on the particle. The electric and magnetic dipole moments induced on the particle can be written as follows [13,19,27–29]:

$$\begin{aligned} \mathbf{p} &= \alpha_{ee}\mathbf{E} + \alpha_{em}\mathbf{B}, \\ \mathbf{m} &= -\alpha_{em}\mathbf{E} + \alpha_{mm}\mathbf{B}. \end{aligned} \tag{3}$$

In Eq. (3), the polarizabilities α_{ee}, α_{em}, and α_{mm} are, respectively, given as follows [13,27,28]:

$$\begin{aligned} \alpha_{ee} &= \frac{i6\pi\varepsilon_0}{k_0^3}a_1^{(1)}, \quad \alpha_{mm} = \frac{i6\pi}{\mu_0 k_0^3}b_1^{(1)}, \\ \alpha_{em} &= -\frac{6\pi}{Z_0 k_0^3}a_1^{(2)}, \end{aligned} \tag{4}$$

where $Z_0 = \sqrt{\mu_0/\varepsilon_0}$ is the wave impedance in vacuum, and the Mie coefficients can be written as [17,28,30,31]

$$\begin{aligned} a_n^{(1)} &= \left[A_n^{(2)}V_n^{(1)} + A_n^{(1)}V_n^{(2)}\right]Q_n, \\ a_n^{(2)} &= \left[A_n^{(1)}W_n^{(2)} - A_n^{(2)}W_n^{(1)}\right]Q_n, \end{aligned}$$

$$b_n^{(1)} = \left[B_n^{(1)} W_n^{(2)} + B_n^{(2)} W_n^{(1)}\right] Q_n,$$
$$b_n^{(2)} = a_n^{(2)}, \tag{5}$$

with

$$A_n^{(j)} = Z_s D_n^{(1)}(x_j) - D_n^{(1)}(x_0),$$
$$B_n^{(j)} = D_n^{(1)}(x_j) - Z_s D_n^{(1)}(x_0),$$
$$W_n^{(j)} = Z_s D_n^{(1)}(x_j) - D_n^{(3)}(x_0),$$
$$V_n^{(j)} = D_n^{(1)}(x_j) - Z_s D_n^{(3)}(x_0),$$
$$Q_n = \frac{\psi_n(x_0)/\xi_n(x_0)}{V_n^{(1)} W_n^{(2)} + V_n^{(2)} W_n^{(1)}}.$$

Here $x_0 = k_0 r_s$, $x_1 = k_1 r_s$, and $x_2 = k_2 r_s$ with r_s being the particle radius. The difference between x_1 and x_2 comes from the particle chirality, as indicated by the definitions of k_1 and k_2. $Z_s = \sqrt{\mu/\varepsilon}$ is the wave impedance of the particle, $\psi_n(x)$ and $\xi_n(x)$ are, respectively, the Riccati–Bessel functions of the first and third kinds, while $D_n^{(1)}(x) = \psi_n'(x)/\psi_n(x)$ and $D_n^{(3)}(x) = \xi_n'(x)/\xi_n(x)$ are the corresponding logarithmic derivatives. It is noted that α_{em} vanishes for a nonchiral particle with $\kappa = 0$ due to the equality of x_1 and x_2, as can be seen from the Mie coefficients given in Eq. (5).

Putting Eq. (3) into Eq. (2), one can write the force expression as

$$\langle \mathbf{F} \rangle = \mathbf{F}_{\text{grad}} + \mathbf{F}_{\text{rad}} + \mathbf{F}_{\text{vor}} + \mathbf{F}_{\text{curl}} + \mathbf{F}_{\text{spin}} + \mathbf{F}_{\text{flow}}, \tag{6}$$

with

$$\mathbf{F}_{\text{grad}} = -\nabla \langle U \rangle,$$
$$\mathbf{F}_{\text{rad}} = \frac{1}{c}(C_{\text{ext}} + C_{\text{recoil}})\langle \mathbf{S} \rangle,$$
$$\mathbf{F}_{\text{vor}} = \mu_0 \text{Re}(\alpha_{em})[\nabla \times \langle \mathbf{S} \rangle],$$
$$\mathbf{F}_{\text{curl}} = C_p c\left[\nabla \times \langle \mathbf{L}_s^p \rangle\right] + C_m c\left[\nabla \times \langle \mathbf{L}_s^m \rangle\right],$$
$$\mathbf{F}_{\text{spin}} = \left[2\omega^2 \mu_0 \text{Re}(\alpha_{em}) - \frac{k_0^5}{3\pi\varepsilon_0^2}\text{Im}(\alpha_{ee}\alpha_{em}^*)\right]\langle \mathbf{L}_s^p \rangle + \left[2\omega^2 \mu_0 \text{Re}(\alpha_{em}) - \frac{k_0^5 \mu_0}{3\pi\varepsilon_0}\text{Im}(\alpha_{mm}\alpha_{em}^*)\right]\langle \mathbf{L}_s^m \rangle,$$
$$\mathbf{F}_{\text{flow}} = \frac{c k_0^4 \mu_0^2}{12\pi}\text{Im}(\alpha_{ee}\alpha_{mm}^*)\text{Im}(\mathbf{E} \times \mathbf{H}^*),$$

where $\mathbf{F}_{\text{grad}}$ is the gradient force, with the optical potential due to the particle-field interaction given by $\langle U \rangle = -\frac{1}{4}\text{Re}(\alpha_{ee})|\mathbf{E}|^2 - \frac{1}{4}\text{Re}(\alpha_{mm})|\mathbf{B}|^2 + \frac{1}{2}\text{Im}(\alpha_{em})\text{Im}(\mathbf{B} \cdot \mathbf{E}^*)$; $\mathbf{F}_{\text{rad}}$ denotes the radiation pressure proportional to the time-averaged Poynting vector $\langle \mathbf{S} \rangle = \frac{1}{2}\text{Re}[\mathbf{E} \times \mathbf{H}^*]$; $\mathbf{F}_{\text{vor}}$ represents the vortex force [13] due to the coupling of the optical vorticity (the curl of the Poynting vector) [32–34] and particle chirality; $\mathbf{F}_{\text{curl}}$ describes the force owing to the curl of the time-averaged SAM densities [35], with $\langle \mathbf{L}_s^p \rangle = \frac{\varepsilon_0}{4i\omega}\mathbf{E} \times \mathbf{E}^*$ and $\langle \mathbf{L}_s^m \rangle = \frac{\mu_0}{4i\omega}\mathbf{H} \times \mathbf{H}^*$; $\mathbf{F}_{\text{spin}}$ comes only from the coupling of the particle chirality with SAM densities; and $\mathbf{F}_{\text{flow}}$ is associated with the alternating flow of the so-called "stored energy" [22]. The cross section $C_{\text{ext}} = C_p + C_m$ is a sum of contributions from the electric and magnetic dipole channels, given by $C_p = k_0 \text{Im}(\alpha_{ee})/\varepsilon_0$ and $C_m = k_0 \mu_0 \text{Im}(\alpha_{mm})$, and the cross section $C_{\text{recoil}} = -\frac{k_0^4 \mu_0}{6\pi\varepsilon_0}[\text{Re}(\alpha_{ee}\alpha_{mm}^*) + |\alpha_{em}|^2]$ is related to the recoil force [26].

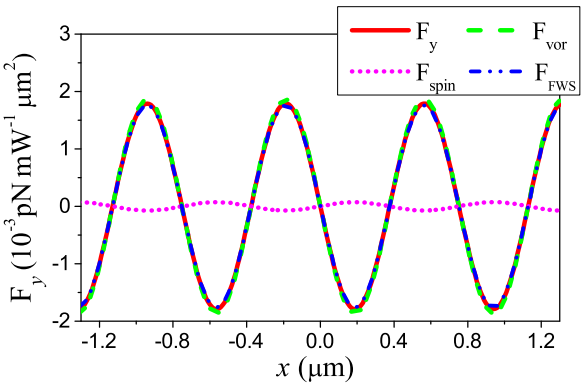

FIG. 3. The terms in Eq. (6) with their y components contributing significantly to the LOF on the chiral particle with $\kappa = 0.3$. The accurate total LOF $\mathbf{F}_{\text{FWS}}$ calculated with the FWS in Fig. 1 is replotted for comparison. All other parameters are the same as those in Fig. 1.

Figure 3 shows the y components of those terms in the optical force defined in Eq. (6) that make significant contributions to the LOF on the chiral particle with $\kappa = 0.3$. Other terms without contributions of the y component; namely, $\mathbf{F}_{\text{grad}}$, $\mathbf{F}_{\text{rad}}$, $\mathbf{F}_{\text{curl}}$, and $\mathbf{F}_{\text{flow}}$, are not plotted in Fig. 3 for clarity. It is unambiguously shown that the LOF comes mostly from the vortex force $\mathbf{F}_{\text{vor}}$, whereas the spin term $\mathbf{F}_{\text{spin}}$ has much smaller contribution to the LOF than the vortex force. Also plotted in Fig. 3 is the total LOF evaluated by Eq. (6), which agrees perfectly with the full-wave numerical result, verifying the analysis within the dipole approximation. As a result, the LOF originates overwhelmingly from the direct interaction of the optical vorticity with the particle chirality. It is noted that the physical origin of the LOF in our case differs from all those reported previously [13,16,29]. Concretely, the LOF on a chiral particle above a substrate is dominated by the electric SAM density and the radiation pressure [13]; the LOF on a chiral particle in evanescent waves is solely ascribed to the transverse SAM density [16]; and the LOF on paired chiral particles with opposite handedness comes mainly from the optical potential gradient formed by the multiple scattering between particles [29].

The time-averaged Poynting vectors displayed in Fig. 4 provide an intuitive understanding of the LOF. The lengths and colors of the arrows represent the magnitudes of the energy flux. For the case of the ordinary particle without chirality, the time-averaged Poynting vectors always maintain the symmetry with respect to $-y$ and $+y$, as visualized in Fig. 4(a), suggesting that photon momenta above and below the particle balance each other, and there yields no LOF acting on the particle. Differently, an interesting result for the chiral particle with $\kappa = 0.3$ can be notably observed in Fig. 4(b), where the total momentum flux scattered to $-y$ and $+y$ is not balanced. As a consequence, a net LOF F_y can now exist and hence pushes the particle along the y direction. We can also find that a vortex of the time-averaged Poynting vectors develops around the chiral particle, which is a manifestation of particle chirality [13]. It is worth noting that the Poynting vectors preserve an asymmetry to the left and right of the

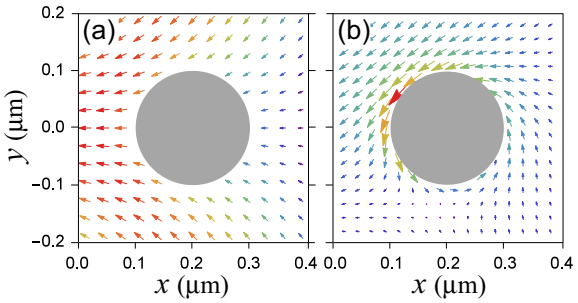

FIG. 4. Time-averaged Poynting vectors for a nanoparticle with (a) $\kappa = 0$, and (b) $\kappa = 0.3$ immersed in the two interfering plane waves. Other parameters are the same as those in Fig. 1 except that the particle is located at $x = 0.2$ μm.

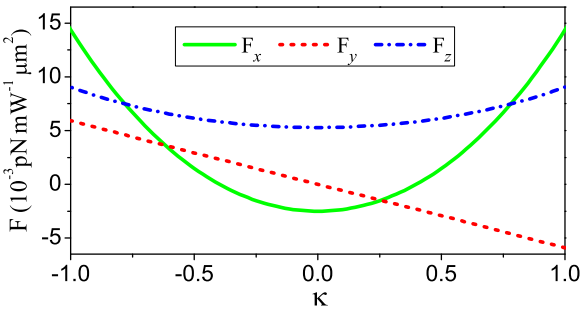

FIG. 5. Optical forces versus the chirality parameter κ. All other parameters are the same as those in Fig. 4.

chiral particle, even for the nonchiral particle. This is because the inhomogeneity of the illuminating field along x direction, and thus gives rise to a transverse gradient force.

We next turn to the dependence of the LOF on chirality parameter κ, as denoted by the red line in Fig. 5, where the particle is located at $x = 0.2$ μm. The LOF is nearly proportional to κ in the range $-1 \leqslant \kappa \leqslant 1$ that may include a lot of chiral materials with an effective chiral parameter [2–4,23,36–38], which takes opposite signs when one switches the helicity and vanishes when the particle is nonchiral. This feature is ascribed to $k_1(\kappa) = k_2(-\kappa)$ because of the symmetry of Mie scattering coefficients with respect to k_1 and k_2. Also, the x and z components of the optical force, arising from the intensity gradient and the radiation pressure, are plotted for comparison, as denoted by the green and blue lines, respectively. It can be clearly seen that the magnitude of LOF is comparable to the forces F_x and F_z when the chirality is large enough, facilitating the chirality sorting of particles. In addition, both F_x and F_z curves exhibit a symmetry with respect to $-\kappa$ and $+\kappa$, irrespective of the handedness.

III. CONCLUSION

In summary, by using the FWS, we have shown that a LOF on chiral nanoparticles can be induced in the direction in which the illumination has neither an intensity gradient nor wave propagation. The LOF can push the particle with opposite helicities towards opposite sides, and, in particular, its magnitude is comparable to that of the gradient force and radiation pressure for the particle with sufficiently large chirality, enabling the potential applications in sorting and separation of chiral molecules and enantiomers [8]. By analytically deriving and evaluating the LOF on chiral particles within the dipole approximation, we have uncovered that the LOF results dominantly from the coupling of the optical vorticity with the particle chirality. Such coupling breaks the lateral symmetry of Poynting vector maps around the particle, and consequently leading to the LOF. These effects are not difficult to be verified experimentally, and also might offer a mechanism for passive chiral spectroscopy.

ACKNOWLEDGMENTS

This work was supported by the China 973 Projects (Grant No. 2013CB632701), the National Natural Science Foundation of China (Grants No. 11274277, No. 11574055, and No. 11574275), Zhejiang Provincial Natural Science Foundation of China (LR16A040001), and the open project of State Key Laboratory of Surface Physics in Fudan University (KF2016_3).

[1] Lord Kelvin, *The Molecular Tactics of a Crystal* (Clarendon Press, Oxford, 1894).
[2] V. K. Valev, J. J. Baumberg, C. Sibilia, and T. Verbiest, Adv. Mater. **25**, 2517 (2013).
[3] Y. Wang, J. Xu, Y. W. Wang, and H. Y. Chen, Chem. Soc. Rev. **42**, 2930 (2013).
[4] L. D. Barron, *Molecular Light Scattering and Optical Activity*, 2nd ed. (Cambridge University Press, Cambridge, 2004).
[5] I. Agranat, H. Caner, and J. Caldwell, Nat. Rev. Drug Discovery **1**, 753 (2002).
[6] G. Subramanian, *Chiral Separation Techniques: A Practical Approach*, 2nd ed. (Wiley-VCH, Weinheim, 2001).
[7] L. A. Nguyen, H. He, and C. P. Huy, Int. J. Biomed. Sci. **2**, 85 (2006).
[8] A. M. Stalcup, Annu. Rev. Anal. Chem. **3**, 341 (2010).
[9] Y. Q. Tang and A. E. Cohen, Phys. Rev. Lett. **104**, 163901 (2010).
[10] D. S. Bradshaw, K. A. Forbes, J. M. Leeder, and D. L. Andrews, Photonics **2**, 483 (2015).
[11] G. Tkachenko and E. Brasselet, Nat. Commun. **5**, 3577 (2014).
[12] G. Tkachenko and E. Brasselet, Nat. Commun. **5**, 4491 (2014).
[13] S. B. Wang and C. T. Chan, Nat. Commun. **5**, 3307 (2014).
[14] F. J. Rodríguez-Fortuño, N. Engheta, A. Martínez, and A. V. Zayats, Nat. Commun. **6**, 8799 (2015).
[15] S. Sukhov, V. Kajorndejnukul, R. R. Naraghi, and A. Dogariu, Nat. Photonics **9**, 809 (2015).
[16] A. Hayat, J. P. B. Mueller, and F. Capasso, Proc. Natl. Acad. Sci. USA **112**, 13190 (2015).
[17] C. F. Bohren and D. R. Huffman, *Absorption and Scattering of Light by Small Particles* (John Wiley and Sons, New York, 1983).

[18] I. V. Lindell, A. H. Sihvola, S. A. Tretyakov, and A. J. Viitanen, *Electromagnetic Waves in Chiral and Bi-Isotropic Media* (Artech House, Boston, 1994).
[19] A. Lakhtakia, V. K. Varadan, and V. V. Varadan, *Time-Harmonic Electromagnetic Fields in Chiral Media* (Springer-Verlag, Berlin, 1989).
[20] M. Yokota, S. L. He, and T. Takenaka, J. Opt. Soc. Am. A **18**, 1681 (2001).
[21] G. Gouesbet and G. Grehan, *Generalized Lorenz-Mie Theories* (Springer-Verlag, Berlin, 2011).
[22] J. D. Jackson, *Classical Electrodynamics*, 3rd ed. (Wiley and Sons, New York, 1999).
[23] G. Cipparrone, A. Mazzulla, A. Pane, R. J. Hernandez, and R. Bartolino, Adv. Mater. **23**, 5773 (2011).
[24] A. Y. Bekshaev, K. Y. Bliokh, and F. Nori, Phys. Rev. X **5**, 011039 (2015).
[25] M. Nieto-Vesperinas, J. J. Sáenz, R. Gómez-Medina, and L. Chantada, Opt. Express **18**, 11428 (2010).
[26] J. Chen, J. Ng, Z. F. Lin, and C. T. Chan, Nat. Photonics **5**, 531 (2011).
[27] K. Ding, J. Ng, L. Zhou, and C. T. Chan, Phys. Rev. A **89**, 063825 (2014).
[28] H. J. Chen, N. Wang, W. L. Lu, S. Y. Liu, and Z. F. Lin, Phys. Rev. A **90**, 043850 (2014).
[29] H. J. Chen, Y. K. Jiang, N. Wang, W. L. Lu, S. Y. Liu, and Z. F. Lin, Opt. Lett. **40**, 5530 (2015).
[30] Q. C. Shang, Z. S. Wu, T. Qu, Z. J. Li, L. Bai, and L. Gong, Opt. Express **21**, 8677 (2013).
[31] Z. S. Wu, Q. C. Shang, and Z. J. Li, Appl. Opt. **51**, 6661 (2012).
[32] L. Allen, S. M. Barnett, and M. J. Padgett, *Optical Angular Momentum* (Institute of Physics Publishing, London, 2003).
[33] M. V. Berry, J. Opt. A **11**, 094001 (2009).
[34] J. Ng, Z. F. Lin, and C. T. Chan, Phys. Rev. Lett. **104**, 103601 (2010).
[35] C. Cohen-Tannoudji, J. Dupont-Roc, and G. Grynberg, *Photons and Atoms: Introduction to Quantum Electrodynamics* (Wiley and Sons, New York, 1989).
[36] J. B. Pendry, Science **306**, 1353 (2004).
[37] A. Canaguier-Durand, J. A. Hutchison, C. Genet, and T. W. Ebbesen, New J. Phys. **15**, 123037 (2013).
[38] M. H. Liu, L. Zhang, and T. Y. Wang, Chem. Rev. (Washington, DC, U.S.) **115**, 7304 (2015).